Transforming growth factor-beta 1 is decreased in remodeling hypertensive bovine pulmonary arteries.

M D Botney, … , K Stenmark, R P Mecham

J Clin Invest. 1992;89(5):1629-1635. https://doi.org/10.1172/JCI115759.

Research Article

The development of pulmonary hypertension in hypoxic newborn calves is associated with a complex pattern of increased tropoelastin and type I procollagen synthesis and deposition by smooth muscle cells in large elastic pulmonary arteries compared to normoxic controls. We examined the possibility that transforming growth factor-beta 1 (TGF-beta 1) may be associated with the production of extracellular matrix protein in this model of pulmonary hypertension. Medial smooth muscle cells in both normotensive and hypertensive vessels, as assessed by immunohistochemistry, were the major source of TGF-beta 1. Staining was confined to foci of smooth muscle cells in the outer media and appeared greater in normotensive than hypertensive vessels. Consistent with the immunohistochemistry, a progressive, age-dependent increase in normotensive pulmonary artery TGF-beta 1 mRNA was observed after birth, whereas TGF-beta 1 mRNA remained at low, basal levels in hypertensive, remodeling pulmonary arteries. These observations suggest that local expression of TGF-beta 1 is not associated with increased extracellular matrix protein synthesis in this model of hypoxic pulmonary hypertension.

Transforming Growth Factor-β_1 Is Decreased in Remodeling Hypertensive Bovine Pulmonary Arteries

Mitchell D. Botney,* William C. Parks,‡ Edmond C. Crouch,§ Kurt Stenmark,‖ and Robert P. Mecham*¶

**Respiratory and Critical Care and ‡Dermatology Divisions, Department of Medicine and §Department of Pathology, Jewish Hospital at Washington University Medical Center, St. Louis, Missouri 63110; ¶Department of Cell Biology, Washington University School of Medicine, St. Louis, Missouri, 63110; and ‖Cardiovascular Pulmonary Laboratory, Webb-Waring Lung Institute, University of Colorado Health Science Center, Denver, Colorado 80262*

Abstract

The development of pulmonary hypertension in hypoxic newborn calves is associated with a complex pattern of increased tropoelastin and type I procollagen synthesis and deposition by smooth muscle cells in large elastic pulmonary arteries compared to normoxic controls. We examined the possibility that transforming growth factor-beta 1 (TGF-β_1) may be associated with the production of extracellular matrix protein in this model of pulmonary hypertension. Medial smooth muscle cells in both normotensive and hypertensive vessels, as assessed by immunohistochemistry, were the major source of TGF-β_1. Staining was confined to foci of smooth muscle cells in the outer media and appeared greater in normotensive than hypertensive vessels. Consistent with the immunohistochemistry, a progressive, age-dependent increase in normotensive pulmonary artery TGF-β_1 mRNA was observed after birth, whereas TGF-β_1 mRNA remained at low, basal levels in hypertensive, remodeling pulmonary arteries. These observations suggest that local expression of TGF-β_1 is not associated with increased extracellular matrix protein synthesis in this model of hypoxic pulmonary hypertension. (*J. Clin. Invest.* 1992. 89:1629–1635.) Key words: vascular remodeling • pulmonary hypertension • elastin • transforming growth factor-beta1 • polymerase chain reaction

Introduction

Hypoxic pulmonary hypertension is characterized by profound remodeling of the pulmonary arterial wall (1). In several animal models, increased extracellular matrix synthesis and deposition is observed in the medial layer of large conducting vessels (2–4). The changes are specific to the pulmonary vasculature since no structural remodeling or increased matrix synthesis is seen in the systemic circulation of animals with pulmonary hypertension. The mechanisms responsible for inducing this altered smooth muscle cell (SMC)[1] phenotype in vivo has not been elucidated; however, recent studies suggest that the phenotype of various matrix producing cells can be modulated by several growth factors.

One of these growth factors, transforming growth factor-beta (TGF-β) is a multipotent peptide growth and differentiation factor (5, 6) that influences extracellular matrix production by mesenchymal cells. For example, TGF-β stimulates in vitro production of fibronectin (7–9), proteoglycan (10), thrombospondin (9), collagen (7, 8, 11) and elastin (12). Increased collagen production is observed after injection of TGF-β into nude mice (13), and increased TGF-β mRNA levels precede the development of pulmonary (14, 15) and hepatic fibrosis (16). Increased TGF-β is also observed in models of vascular remodeling including development of pulmonary hypertension after air embolism (17), repair of arterial injury after carotid endarterectomy (18), and development of systemic hypertension after salt and mineralocorticoid administration (19).

Neonatal bovine hypoxic pulmonary hypertension provides a well-characterized model to identify factors that modulate vascular remodeling. Newborn calves placed at a simulated altitude of 4,300 m demonstrate a progressive increase in pulmonary artery pressure compared with control calves (20). For example, between days 2 and 15 pulmonary artery pressure rises from 67 to 101 mmHg while control calf pulmonary artery pressure remains around 30 mmHg. Furthermore, 100% O_2 lowers the elevated pulmonary artery pressure after 2 d of simulated high altitude, but O_2 reversibility is lost after exposure to high altitude for 15 d. This irreversible increase in pulmonary artery pressure is associated with increased connective tissue deposition by pulmonary artery medial SMC lying between the elastic lamellae of large conducting vessels (4, 21, 22). Interestingly, non-matrix producing SMC are found in the outer media of both normal and hypertensive vessels. These cells occurred as broad circumferential bands in normal vessels and as nodular foci in hypertensive vessels (22). Little is known, however, about the function of these non-matrix producing cells or what factors induce this complex pattern of exuberant vascular remodeling.

To begin examining the role of various growth factors in stimulating vascular remodeling in this model of pulmonary hypertension, we used immunohistochemistry and reverse transcription–polymerase chain reaction (RT-PCR) amplifica-

This paper was presented in part at the Aspen Lung Conference, Aspen, Colorado, May, 1990.

Address correspondence to Mitchell Botney, M.D., Respiratory and Critical Care Division, Jewish Hospital, 216 S. Kingshighway Boulevard, St. Louis, MO 63110.

Received for publication 15 January 1991 and in revised form 3 December 1991.

J. Clin. Invest.

0021-9738/92/05/1629/07 $2.00
Volume 89, May 1992, 1629–1635

1. *Abbreviations used in this paper:* MMLV, Moloney murine leukemia virus; PCR, polymerase chain reaction; RT-PCR, reverse transcription–PCR; SMC, smooth muscle cells; TGF-β, transforming growth factor-β.

tion to study the spatial distribution and temporal changes of TGF-β_1 expression in normal and hypertensive pulmonary arteries.

Methods

Materials. Moloney murine leukemia virus (MMLV) reverse transcriptase, affinity-purified biotin-conjugated goat anti-rabbit IgG and horseradish peroxidase-streptavidin (10:1 ratio) were purchased from Bethesda Research Laboratories (Gaithersburg, MD). pGEM-4Z DNA and RNasin was purchased from Promega Biotec (Madison, WI). $\alpha[^{32}P]$dCTP and $\gamma[^{32}P]$dATP was purchased from ICN Pharmaceuticals, Inc. (Irvine, CA). Rabbit polyclonal anti-human TGF-β_1 antibody (23) was kindly supplied by K. Flanders (National Institutes of Health, Bethesda, MD). Human TGF-β_1 cDNA (24) was kindly provided by R. Derynck (Genentech, Inc., South San Francisco, CA).

Animal model. Newborn calves were maintained at an ambient altitude of 1,500 m for 24 h and then placed at a simulated altitude of 4,500 m. Age-matched control calves were maintained at ambient altitude. Calves placed at the simulated high altitude demonstrate an immediate rise in pulmonary artery pressure. Within 2 wk these calves develop suprasystemic pulmonary artery pressures which are maintained even in the presence of oxygen breathing. The physiological consequences of high altitude are largely confined to the pulmonary vasculature since no significant changes in pressure is observed in the systemic vasculature (20).

To characterize the changes occurring in the pulmonary vessels, proximal intralobar pulmonary arteries and thoracic aortas were removed from normal calves or age-matched calves with hypoxic pulmonary hypertension. Immediately after euthanasia with sodium pentobarbital, both lungs and the thoracic aorta from each calf were resected. One lung was perfused at physiologic pressure via the trachea and pulmonary artery with phosphate-buffered formalin. The lobar pulmonary artery between branches 1 and 6 from the other lung was resected and immediately frozen on dry ice for RNA extraction or processed for SMC explant culture. The thoracic aorta was similarly processed for RNA extraction.

Immunohistochemistry. Proximal intralobar pulmonary artery segments were fixed in phosphate-buffered formalin for 6 h and subsequently dehydrated in sequential 30%, 50%, and 70% ethanol washes. Tissues were then embedded and prepared for immunoperoxidase staining as described previously (20). All tissue samples were pretreated with hyaluronidase (1 mg/ml in PBS) for 30 min at 37°C after blocking endogenous peroxidase with 0.3% (vol/vol) H_2O_2 in methanol for 20 min at room temperature. Nonspecific immunoglobulin binding sites were blocked with normal goat serum. Sections were subsequently incubated overnight at 4°C with rabbit polyclonal anti-human TGF-β antibody or rabbit immunoglobulin (negative control). Sections were then incubated for 30 min with affinity-purified biotin-conjugated goat anti-rabbit IgG (1:1,600 dilution), washed, and incubated for 30 min with horseradish peroxidase-streptavidin (1:400 dilution). Immunoglobulin complexes were then visualized by incubation with 3,3'-diaminobenzidine (0.5 mg/ml in 50 mM Tris-HCl, pH 7.4) and 3% H_2O_2. Sections were washed, dehydrated, mounted in Permount, and examined by light microscopy.

RNA. RNA from the resected arteries was isolated by homogenization in guanidine thiocyanate and isopycnic centrifugation through cesium chloride (25). RNA quantity was determined by ultraviolet spectrophotometry. Quality was assessed by ethidium bromide staining following electrophoresis under denaturing conditions (21).

Preliminary experiments with known quantities of a RNA template were performed to determine if the product of sequential reverse-transcription and polymerase chain reaction amplification was sensitive to the initial input RNA copy number. pGEM-4Z DNA was linearized with SspI restriction enzyme, and RNA of ~ 750 nucleotides was transcribed using T7 RNA polymerase. The quantity of RNA was determined by ultraviolet spectrophotometry. This in vitro transcribed RNA migrated as a single band during electrophoresis in a formaldehyde agarose gel (data not shown).

U937 cells were grown to confluency in 10% FCS. Total cellular RNA was purified by homogenization in guanidine thiocyanate and isopycnic centrifugation through cesium chloride. RNA quantity was determined by ultraviolet spectrophotometry.

Reverse transcription–polymerase chain reaction amplification. Oligomeric deoxynucleotide primers were synthesized by the β-cyanoethyl phosphoramidite method and gel purified as previously described (21). Pairs of oligomeric primers were designed to amplify an ~ 500 nucleotide region of the RNA of interest. For pGEM-4Z RNA, primer 19R (5'-CCTGGCGTTACCCAACTTAATTCGCC-3') is complementary to nucleotides 2661 through 2635 while primer 12 (5'-CAAATAGGGGTTCCGCGCACATTTC-3') corresponds to nucleotides 2216 through 2241 of the pGEM-4Z cDNA. For TGF-β_1 mRNA, primer 106R (5'-GTCAATGTACAGCTGCCGCACGCA-3') is complementary to nucleotides 1748 through 1724 while primer 105 (5'-AACACATCAGAGCTCCGAGAAGCG-3') corresponds to nucleotides 1248 through 1272 (24). The specificity of these primers for TGF-β_1 is suggested by the high degree of base-pair mismatch between these primers and human TGF-β_2 (26), human TGF-β_3 (27), chick TGF-β_4 (28), and xenopus TGF-β_5 (29). In addition, analysis of the "best" matched base-pairing between the primers and the non–TGF-β_1 sequences revealed either incorrect primer orientation, thereby preventing PCR amplification, or predicted a PCR amplification product length other than the observed 500 nucleotides. Oligomeric primers 380R and 381, used for RT-PCR amplification, correspond to highly homologous regions in both mouse (30) and human glyceraldehyde-3-phosphate dehydrogenase (31) cDNA. Primer 380R (5'-GCCTGCTTCACCACCTTCTTGATGTC-3') was complementary to nucleotides 855 through 830 while primer 381 (5'-CTGAGAACGGGAAGCTTGTCATCAA-3') was complementary to nucleotides 245 through 270. Southern blot analysis of the RT-PCR product was performed with oligomer 385 (5'-CTCATGACCACAGTCCAT-3'), complementary to a third highly homologous region between nucleotides 581 through 597 in both the mouse and human glyceraldehyde-3-phosphate dehydrogenase (G3PDH) cDNA.

pGEM-4Z or total vascular RNA samples were incubated with 200 U MMLV reverse transcriptase in a 20-μl vol containing reverse transcriptase buffer (0.25 M Tris-HCl, pH 8.3, 0.375 M KCl, 15 mM $MgCl_2$, 50 mM dithiothreitol), 10 U RNasin, 10 pmol of appropriate complementary primer (19R, 106R, or 380R) and 40 mmol each dATP, dCTP, dGTP, and TTP for 1 h at 37°C. Samples were heated at 94°C, and 80 μl PCR buffer (50 mM KCl, 3 mM $MgCl_2$, 160 μmol each dATP, dCTP, dGTP, and TTP, 0.01% (wt/vol) gelatin, 10 mM Tris (pH 8.3), 40 pmol of the first extension primer and 50 pmol of the second primer, and 5 U Taq DNA polymerase) was added. Cycling consisted of denaturing at 94°C for 1 min, annealing at 50°C for 2 min, and extension at 72°C for 3 min. Aliquots were removed at the end of a cycle and immediately placed on ice. Each sample was fractionated by 1% agarose electrophoresis, transferred to nitrocellulose, and analyzed by Southern blot analysis. Nick translated pGEM-4Z or TGF-β_1 cDNA, or 5'-labeled oligomer 385 were prepared as previously described (21). Autoradiograms were scanned by a Scanning Densitometer (GS300; Hoefer Scientific Instruments, San Francisco, CA) and the data are expressed as arbitrary units.

Results

Immunohistochemical studies. Sections from formalin-fixed normotensive or hypertensive proximal intralobar pulmonary arteries were incubated with rabbit polyclonal anti-TGF-β_1 antibody. This antibody recognizes an intracellular form of TGF-β_1 (23) and allows the localization of TGF-β_1 protein synthesis in these arteries. Positively stained cells in both normotensive and hypertensive vessels were unevenly distributed throughout

the media, appearing as intensely staining clusters compared to the surrounding tissue (Fig. 1, *A* and *B*). These TGF-β_1–positive clusters were dispersed throughout the outer two-thirds of the medial layer in normotensive vessels in contrast to previous studies which had demonstrated tropoelastin synthesis in the inner one-third of the media (22). Elastin lamellae were not apparent in these immunopositive clusters, similar to the previously identified non–matrix producing clusters of SMC. Relatively fewer clusters of cells in hypertensive vessels stained for TGF-β_1 and these were localized to the media adjacent to the adventitia. Normotensive endothelial cells stained weakly while staining appeared more intense in endothelial cells from hypertensive vessels. In both normotensive and hypertensive vessels intense staining was associated with cells of the vasa vasorum. No cells were immunoreactive in sections incubated with normal rabbit serum as the primary antibody (data not shown).

Reverse transcription–polymerase chain reaction amplification. Initial studies suggested TGF-β_1 mRNA levels in normal and hypertensive pulmonary arteries were below the sensitivity of Northern blot analysis. Therefore, RT-PCR amplification was performed to determine relative mRNA levels in these vessels. Preliminary experiments with known quantities of pGEM-4Z RNA were performed to determine if the quantity of double-stranded DNA produced by sequential RT-PCR accurately reflected initial RNA concentration. The studies were also designed to determine if the RT-PCR assay was sufficiently sensitive to discriminate between small differences in the number of RNA molecules as well as capable of accurately reflecting a large range of initial RNA concentrations. 10^4, 10^6, and 10^8 copies of pGEM-4Z RNA in a total vol of 100 μl were reverse-transcribed with sequence-specific primer 19R, and the resulting cDNA was cyclically amplified after addition of primer 12. Aliquots of the amplification mixture were sampled at the end of every third cycle of amplification and fractionated through 1% agarose. PCR product was not visible after staining with ethidium bromide at low cycle numbers, and therefore, Southern blot analysis was performed using a ^{32}P-labeled pGEM-4Z DNA probe. With 10^8 copies of pGEM-4Z RNA, an exponential increase in signal strength was observed with increasing cycle number (Fig. 2 *A*). With lower concentrations of RNA (10^6 and 10^4 copies per reaction) autoradiographic signals were seen only at higher cycle numbers. With 15 cycles of amplification autoradiographic signal strength was strongest using the highest concentration of RNA and weakest with the lowest concentration of RNA. A graphic representation of a densitometry scan of the autoradiogram is shown in Fig. 2 *B*. These data indicated concordance between the product of RT-PCR and the initial quantity of RNA.

To determine if RT-PCR was sensitive to small differences in RNA concentration, 3×10^7 and 1.5×10^8 copies of RNA were reverse transcribed, amplified, and analyzed as above. As shown in Fig. 3, *A* and *B*, RT-PCR was able to detect a fivefold relative difference in the initial quantity of RNA.

The preliminary experiments with RT-PCR described above (Figs. 2 and 3) were performed with a homogenous prepa-

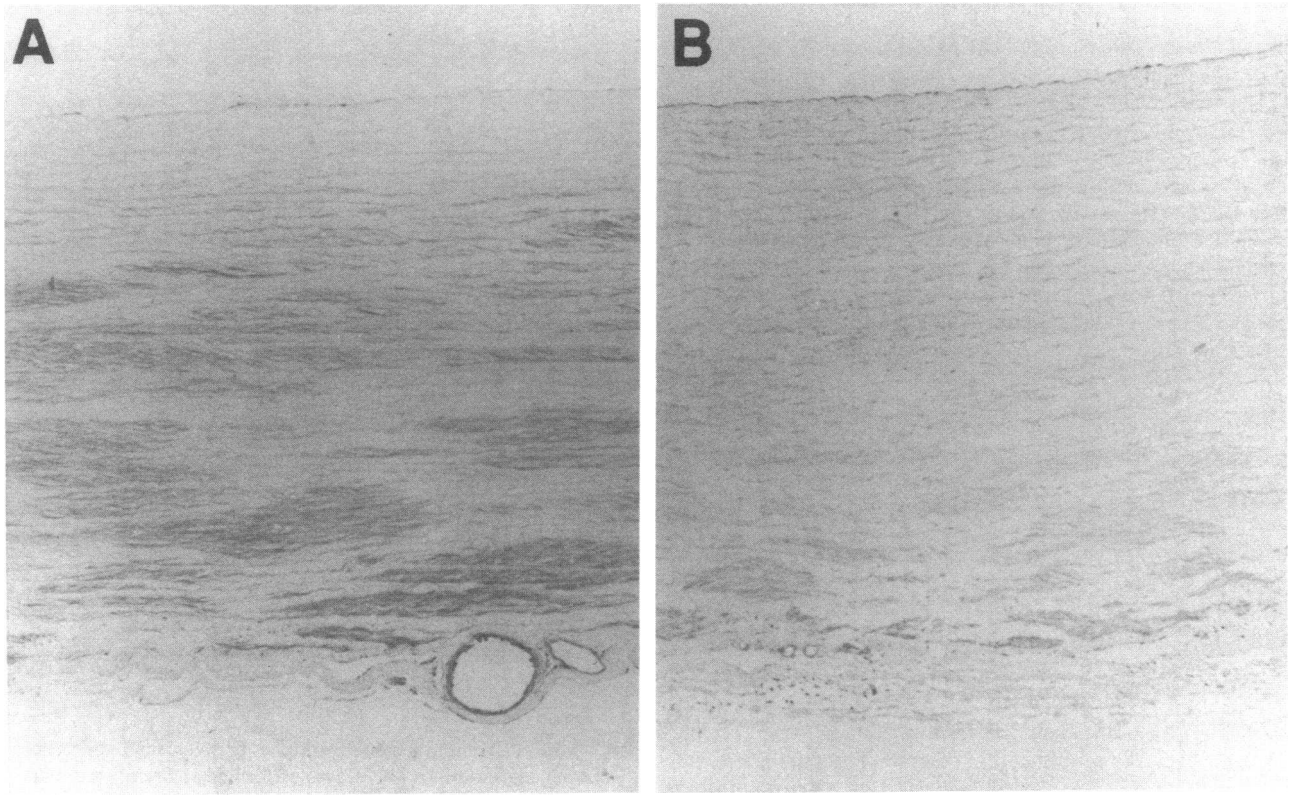

Figure 1. Immunohistochemical stain for TGF-β_1 in pulmonary arteries. Immunohistochemical stain showing location of TGF-β_1 protein in 15-d-old formalin-fixed pulmonary arteries. The primary antibody is a rabbit polyclonal anti-human TGF-β_1 IgG (1:750 dilution) (23). The micrographs are oriented so that the lumen is at the top. TGF-β_1 staining localizes to foci of cells in the outer two-thirds of the media in normal vessels (*A*) and in the media adjacent to the adventitium in hypertensive vessels (*B*). These foci are similar to previously described foci of non–matrix producing SMC (22) (×100).

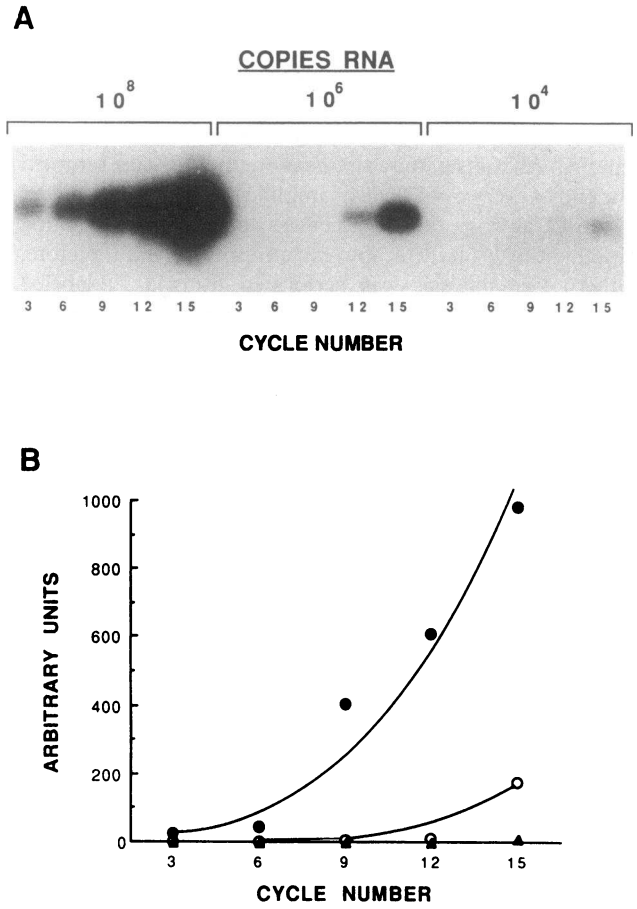

Figure 2. RT-PCR accurately reflects low numbers of RNA over wide range of concentrations. RNA was transcribed from pGEM-4Z plasmid, quantitated by ultraviolet spectrophotometry, and serially diluted. Reverse transcription was performed using sequence-specific extension primer 19R and MMLV reverse transcriptase. Polymerase chain reaction amplification was performed using a second sequence-specific extension primer 12 and Taq DNA polymerase. Aliquots of the amplification mixture were removed after every third cycle, fractionated through 1% agarose, transferred to nitrocellulose, and analyzed by Southern blot technique. Three different RNA concentrations are shown: 10^8, 10^6, and 10^4 molecules RNA per reaction mixture. (*A*) Autoradiogram shows RT-PCR signal strength increases with increasing cycle number. After 15 cycles RT-PCR signal strength is greatest with 10^8 initial copies of RNA and weakest with 10^4 copies of RNA. (*B*) Graphic representation of densitometry scan of autoradiogram. (●) 10^8 copies RNA, (○) 10^6 copies RNA, (▲) 10^4 copies RNA initially.

ration of pGEM-4Z RNA rather than with a heterogenous mixture of RNA species. To determine if RT-PCR accurately reflected different amounts of TGF-β_1 mRNA in total cellular RNA, RT-PCR was performed with serially diluted total cellular RNA purified from cells of the U937 monocyte-derived cell line and TGF-β_1 specific primers. Decreasing signal strength was observed with decreasing concentrations of U937 cell RNA after 9 cycles of amplification (Fig. 4). The difference in signal strength observed comparing lanes 2 and 3, representing 0.5 and 1.0 μg initial RNA, respectively, indicated RT-PCR can distinguish a twofold relative difference in a particular RNA species amidst a complex RNA mixture.

Specificity of RT-PCR was demonstrated on autoradiograms by the appearance of a single band at the predicted molecular weight of 500 bp. Typically, with 1 μg total RNA, only 12–18 amplification cycles were required to see the RT-PCR product by Southern blot analysis. With 25–60 cycles, additional high molecular weight bands were seen with ethidium bromide staining and on Southern blot autoradiograms. Consequently, all PCR amplifications were kept below 20 cycles.

To examine the relative amounts of TGF-β mRNA in proximal intralobar pulmonary arteries, mRNA was purified from normal and hypertensive vessels obtained from 15-d-old calves. 1 μg of total cellular RNA was reverse transcribed to a cDNA using primer 106R. Polymerase chain reaction amplification was performed, and aliquots were removed after every third cycle. After electrophoresis and transfer to nitrocellulose, Southern blot analysis was performed using a human ^{32}P-labeled TGF-β_1 cDNA probe. The 500 nucleotide size of the RT-PCR product was confirmed by comparison to the migration of DNA molecular weight markers. Although an increase in signal strength was observed with increasing cycle number for both RNA samples, the overall signal strength was diminished in the hypertensive sample compared to control (Fig. 5 *A*). Ethidium bromide staining (Fig. 5 *B*) demonstrated that

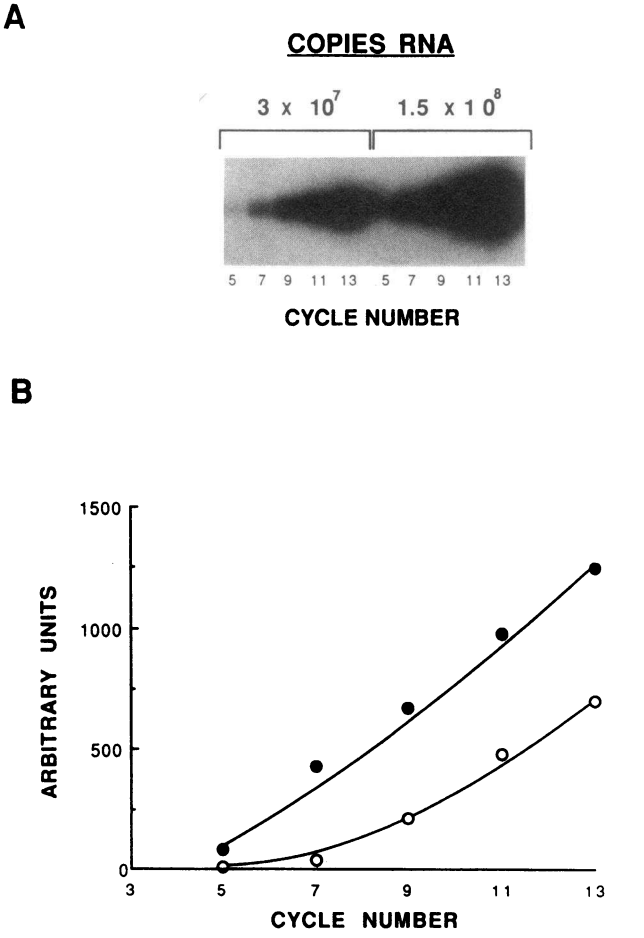

Figure 3. RT-PCR accurately discriminates between small differences in RNA concentrations. RT-PCR was performed as described in Fig. 1. Initial RNA concentrations were 3×10^7 and 1.5×10^8. (*A*) Autoradiogram shows RT-PCR signal strength increases with increasing cycle number but after any given cycle signal strength is greater with 1.5×10^8 initial copies of RNA than with 3×10^7 copies. (*B*) Graphic representation of densitometry scan of autoradiogram. (●) 3×10^8 copies RNA, (○) 1.5×10^7 copies RNA initially.

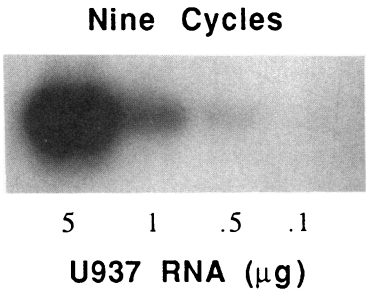

Figure 4. RT-PCR accurately reflects TGF-β_1 levels in total cellular RNA. RT-PCR was performed with serially diluted total cellular RNA purified from cells of the U937 monocyte-derived cell line. Reverse transcription was performed using sequence-specific extension primer 106R and MMLV reverse transcriptase. Polymerase chain reaction amplification was performed using a second sequence-specific extension primer 105 and Taq DNA polymerase. Decreasing signal strength is observed with decreasing concentrations of U937 cell RNA after nine cycles of amplification. The difference in signal strength observed comparing lanes *2* and *3*, representing 0.5 and 1.0 μg initial RNA, respectively, indicates RT-PCR has the ability to distinguish a twofold difference in a particular RNA species amidst a complex RNA mixture.

RNA from the normal and hypertensive intralobar pulmonary arteries was of comparable quality and concentration. RT-PCR analysis indicated equivalent amounts of the glyceraldehyde-3-phosphate dehydrogenase mRNA, used as an indicator of constitutive gene expression, in both samples (Fig. 5 *A*).

The relative decrease in TGF-β_1 signal strength between normal and hypertensive pulmonary arteries was also evident when pulmonary artery RNA from newborn, 2-d, and 8-d high altitude and age-matched control calves were studied by RT-PCR amplification. Elevated signal strength as a function of increasing cycle number was again observed, but, for ease of comparison, only the product of 18 cycles of amplification is shown in Fig. 6. In normal animals, TGF-β_1 mRNA levels increased with age. In comparison, TGF-β_1 mRNA was markedly decreased in samples from 2-d and 8-d hypertensive calves, respectively. These data indicate that TGF-β_1 mRNA steady-state levels remain at low, basal levels in hypertensive

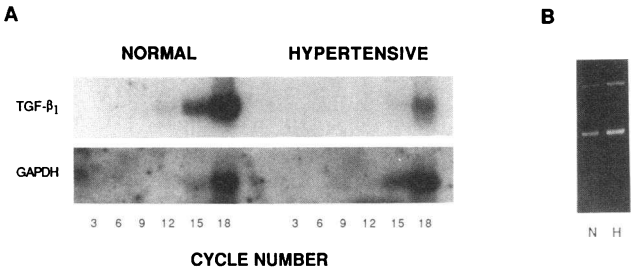

Figure 5. TGF-β_1 RT-PCR signal strength is markedly different in RNA from normal and hypertensive pulmonary arteries. RNA was purified from normal or hypertensive pulmonary arteries. RT-PCR was performed as described in Fig. 3 using 1 μg RNA and TGF-β_1 or G3PDH specific primers. Aliquots of the amplification mixture were removed after every third cycle, fractionated through 1% agarose, transferred to nitrocellulose, and analyzed by Southern blot technique. (*A*) Autoradiogram shows RT-PCR signal strength for TGF-β_1 is greatest in RNA from normal compared to RNA from hypertensive pulmonary arteries while similar RT-PCR signals for G3PDH are seen. (*B*) Ethidium bromide gel of normotensive (lane *1*) and hypertensive pulmonary artery (lane *2*) RNA (5 μg each) used for RT-PCR.

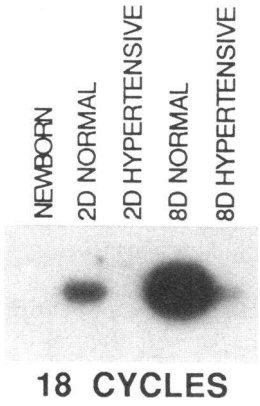

Figure 6. Age-dependent increase in TGF-β_1 mRNA from pulmonary arteries. Pulmonary artery RNA from newborn calves and 2- and 8-d-old high altitude or age-matched control calves was studied by RT-PCR analysis as described in Fig. 3. The autoradiogram after 18 cycles of amplification is shown. TGF-β_1 signal strength increases with age in the control calves but remains at basal levels in hypertensive pulmonary arteries.

pulmonary arteries compared to rising levels in normal pulmonary arteries.

In the bovine model of hypoxic pulmonary hypertension, the systemic circulation shows no significant increase in vascular pressure and does not undergo the extensive remodeling seen in the pulmonary circulation (4). The thoracic aorta, therefore, provides a convenient internal control for making comparisons with remodeling pulmonary arteries. Interestingly, when the steady-state levels of TGF-β_1 mRNA were determined in RNA isolated from the thoracic aorta from three separate 15-d control and hypoxic calves, the hypoxic animals again had lower levels compared with the controls (Fig. 7).

Discussion

The development of pulmonary hypertension in hypoxic newborn calves is characterized by a complex pattern of increased tropoelastin and type I procollagen synthesis and deposition by SMC in large elastic pulmonary arteries compared to normoxic controls. These matrix producing cells lie between elastic lamellae with foci of non–matrix producing SMC present in the outer media in both control and hypertensive vessels. Thus, remodeling in this animal model of pulmonary hypertension occurs in discrete locations and permits the examination of spatial and temporal relationships between growth or differentiation factors and matrix production. We examined the in vivo role of TGF-β_1 in pulmonary artery remodeling by comparing the pattern of immunohistochemical staining for TGF-β_1 protein with the previously described pattern of tropoelastin synthesis in normal and hypertensive vessels (22). In that study, clusters of cells in both normal and hypertensive vessels stained positively for α-smooth muscle actin, desmin, and vimentin, consistent with a smooth muscle cell phenotype. These clusters of cells did not contain positive signal for tropo-

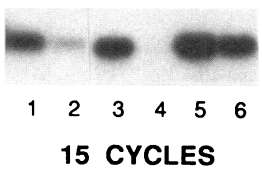

Figure 7. TGF-β_1 mRNA decreased in thoracic aortas from three calves with pulmonary hypertension. Thoracic aorta RNA from 15-d-old calves with normal or hypertensive pulmonary arteries was studied by RT-PCR analysis as described in Fig. 3. The autoradiogram after 15 cycles of amplification is shown. TGF-β_1 signal strength is decreased in RNA from thoracic aortas of three different calves with pulmonary hypertension (lanes *2*, *4*, and *6*) compared with three calves with normal pulmonary arteries (lanes *1*, *3*, and *5*).

elastin mRNA nor did they contain elastin fibers. In this study, immunoreactivity for TGF-β_1 also was found in large foci of medial cells. The foci of TGF-β_1 immunoreactivity observed in this series of experiments were found in similar locations and numbers as the previously described foci of non-matrix producing cells, and did not contain elastin fibers. Therefore, the foci of TGF-β_1 immunoreactivity appear to coincide with the foci of non-matrix producing cells. Although the distribution was nonuniform, the number of immunoreactive foci appeared greater in normotensive than hypertensive vessels.

We used sequential reverse transcription–polymerase chain reaction amplification to compare the relative differences in TGF-β_1 mRNA steady-state levels in normally developing and hypertensive pulmonary arteries. This technique was used because our initial studies suggested TGF-β_1 mRNA levels in these vessels were below the sensitivity of Northern blot analysis. Preliminary experiments using purified pGEM-4Z RNA as a template for RT-PCR indicated reliable concordance between the final double-stranded DNA product of RT-PCR and initial RNA concentration. Preliminary experiments also demonstrated that this technique could detect as few as 100 copies of RNA per microliter and that it was sufficiently sensitive to discriminate between a fivefold difference in initial RNA concentrations. Similar results were obtained using total cellular RNA obtained from U937 cells. Specificity of amplification was enhanced by the use of paired TGF-β_1–specific primers (see Methods), Southern blot analysis using a ^{32}P-labeled TGF-β_1 cDNA probe (which demonstrated an appropriately sized RT-PCR product), and a low number of PCR amplification cycles. Fewer cycle numbers alleviated the problem of extraneous high molecular weight bands appearing at high cycle numbers. In addition, we observe consistent decreases in the PCR signal ratio between two samples with increasing cycle number, though this ratio theoretically remains constant with increasing cycle number. Fewer cycles minimizes the influence of substrate depletion and other artifacts that limit efficient amplification, and consequently, reduce PCR signal ratios at higher template copy numbers (32, 33). Therefore, the relative differences in PCR signal strength between two different samples at any given cycle number likely represent a minimum value, implying even larger relative differences between samples if non-PCR analytical techniques were employed. Finally, in addition to enhancing the signal-to-noise ratio for low abundance mRNAs, RT-PCR has the advantage of requiring small amounts of material. This technique conserves the limited amount of RNA obtained from small or fibrous tissue samples. When RT-PCR was applied to RNA isolated from normal neonatal pulmonary arteries, an age-dependent increase in TGF-β_1 mRNA levels was observed. In contrast, no increase in TGF-β_1 mRNA was evident in remodeling hypertensive pulmonary arteries or, remarkably, in the non-remodeling normal thoracic aortae from animals with pulmonary hypertension.

The absence of an age-dependent increase in TGF-β_1 mRNA in hypertensive vessels, while tropoelastin production is increased, along with decreased TGF-β_1 mRNA in non-remodeling normal thoracic aortae from animals with pulmonary hypertension, and the discordant spatial relationship between TGF-β_1 immunoreactivity (Fig. 1) and tropoelastin mRNA (22) suggests that TGF-β_1 does not influence tropoelastin production by vascular cells in this model. This is in contrast to in vitro studies in which exogenous TGF-β_1 stimulated tropoelastin synthesis two- to threefold by cultured neonatal rat lung fibroblasts (34) or porcine SMC (12). However, whether a growth factor is capable of inducing an alteration in phenotype, such as stimulate extracellular matrix production, may be a function of conditions associated with in vitro culture (35) or the net effect of the entire set of growth factors located in the cellular microenvironment (36, 37). While the discovery that TGF-β_1 induces extracellular matrix production in cultured cells is potentially important, cell culture studies may not always reflect in vivo remodeling.

Our results also differ from several in vivo experiments that have documented a positive correlation between TGF-β_1 levels and extracellular matrix production (13–16). However, unlike our hypoxic pulmonary hypertension model, these models have a significant inflammatory component. Supporting a role for TGF-β_1 in extracellular matrix production associated with inflammation is a recent study detecting TGF-β_1 mRNA in human fibrosing skin conditions associated with marked inflammation whereas TGF-β_1 mRNA was undetectable in progressive systemic sclerosis, a non-inflammatory fibrosing skin condition (38). In addition, increased TGF-β_1 mRNA levels were observed within hours after balloon angioplasty (18), at a time when SMC enter S phase (39), whereas increased fibronectin and collagen mRNA levels correlated with the formation of neointima 1 wk later. Thus, our data are consistent with the suggestion that some other mechanism(s) is directly responsible for the exuberant tropoelastin production observed in this hypoxic hypertensive model of vascular remodeling (4).

The absence of a normal increase in TGF-β_1 mRNA in hypertensive arteries may be explained by fewer foci of SMC producing TGF-β_1 in hypertensive vessels compared to normal vessels rather than a decrease in steady-state mRNA levels per cell. This implies a more subtle regulation of growth factor production in response to hypoxia or hypertension than a direct effect on TGF-β_1 gene expression and is consistent with in vitro experiments in which hypoxia had no effect on TGF-β_1 mRNA levels in cultured human endothelial cells (40). While hypoxia may not directly inhibit TGF-β_1 gene expression, decreased steady-state levels of TGF-β_1 mRNA in normotensive, non-remodeling thoracic aortas from calves with pulmonary artery hypertension suggests that the mechanism responsible for decreased TGF-β_1 mRNA is not specific for the hypertensive pulmonary artery.

While our observations do not suggest a direct role for TGF-β_1 in the stimulation of tropoelastin production in neonatal bovine hypoxic pulmonary hypertension, the progressive, age-dependent increase in normal pulmonary artery TGF-β_1 mRNA after birth suggests an important role for TGF-β_1 in normal vascular development. Within the first hours after birth an acute increase in lumen diameter is associated with a decrease in SMC diameter ("thinning") without reduction in SMC mass (41, 42). In the following weeks the SMCs of the elastic pulmonary arteries grow and show an increase in myofilament concentration and a switch from "synthetic" to "contractile" phenotype. Whether TGF-β_1 production or some other feature of these foci contributes to this normal SMC growth or change in phenotype is unknown.

In summary, on the basis of previous in vitro and in vivo experiments indicating TGF-β_1 stimulates production of several extracellular matrix proteins, we used a model of pulmonary hypertension which is characterized, in part, by exuberant matrix production though without an inflammatory component, to study the relationship between TGF-β_1 and tropoelas-

tin production in vivo. Both the spatial distribution of TGF-β_1 immunoreactivity, and similar levels of TGF-β_1 mRNA in remodeling hypertensive pulmonary arteries or normal thoracic aortae from animals with pulmonary hypertension compared to normal animals, suggest local expression of TGF-β_1 is not directly associated with the development of hypoxic pulmonary hypertension or the regulation of tropoelastin synthesis. However, this study does not exclude the possibility that other isoforms of TGF-β participate in the synthesis of tropoelastin and in the pathogenesis of pulmonary hypertension.

Acknowledgments

We thank D. Parghi and J. Roby for expert technical assistance.

This work was supported by grants HL-29594 and HL-02425 from the National Institutes of Health. M. D. Botney is a recipient of a Physician-Scientist Award from the National Institutes of Health.

References

1. Wagenvoort, C. A., and N. Wagenvoort. 1977. Pathology of Pulmonary Hypertension. John Wiley & Sons, Inc., New York.

2. Meyrick, B., and L. Reid. 1980. Hypoxia-induced structural changes in the media and adventitia of the rat hilar pulmonary artery and their regression. *Am. J. Pathol.* 100:151–178.

3. Poiani, G. J., C. A. Tozzi, S. E. Yohn, R. A. Pierce, S. A. Belsky, R. A. Berg, S. Y. Yu, S. B. Deak, and D. J. Riley. 1990. Collagen and elastin metabolism in hypertensive pulmonary arteries of rats. *Circ. Res.* 66:968–978.

4. Mecham, R. P., L. A. Whitehouse, D. S. Wrenn, W. C. Parks, G. L. Griffin, R. M. Senior, E. C. Crouch, K. R. Stenmark, and N. F. Voelkel. 1987. Smooth muscle-mediated connective tissue remodeling in pulmonary hypertension. *Science (Wash. DC).* 237:423–426.

5. Massague, J. 1987. The TGF-β family of growth and differentiation factors. *Cell.* 49:437–438.

6. Sporn, M. B., A. B. Roberts, L. M. Wakefield, and R. K. Assoain. 1986. Transforming growth factor-β: biological function and chemical structure. *Science (Wash. DC).* 233:532–534.

7. Ignotz, R. A., and J. Massague. 1986. Transforming growth factor-β stimulates the expression of fibronectin and collagen and their incorporation into the extracellular matrix. *J. Biol. Chem.* 261:4337–4345.

8. Ignotz, R. A., T. Endo, and J. Massague. 1987. Regulation of fibronectin and type I collagen mRNA levels by transforming growth factor-β. *J. Biol. Chem.* 262:6443–6446.

9. Penttinen, R. P., S. Kobayashi, and P. Bornstein. 1988. Transforming growth factor β increases mRNA for matrix proteins both in the presence and in the absence of changes in mRNA stability. *Proc. Natl. Acad. Sci. USA.* 85:1105–1108.

10. Chen, J. K., H. Hoshi, and W. L. McKeehan. 1987. Transforming growth factor type β specifically stimulates synthesis of proteoglycan in human adult arterial smooth muscle cells. *Proc. Natl. Acad. Sci. USA.* 84:5287–5291.

11. Fine, A., and R. H. Goldstein. 1987. The effect of transforming growth factor-β on cell proliferation and collagen formation by lung fibroblasts. *J. Biol. Chem.* 262:3897–3902.

12. Liu, J. M., and J. M. Davidson. 1988. The elastogenic effect of recombinant transforming growth factor-beta on porcine aortic smooth muscle cells. *Biochem. Biophys. Res. Commun.* 154:895–901.

13. Roberts, A. B., M. B. Sporn, R. K. Assoian, J. M. Smith, N. S. Roche, L. M. Wakefield, U. I. Heine, L. A. Liotta, V. Falanga, J. H. Kerhl, and A. S. Fauci. 1986. Transforming growth factor type β: rapid induction of fibrosis and angiogenesis in vivo and stimulation of collagen formation in vitro. *Proc. Natl. Acad. Sci. USA.* 83:4167–4171.

14. Khalil, N., O. Bereznay, M. Sporn, and A. H. Greenberg. 1989. Macrophage production of transforming growth factor β and fibroblast collagen synthesis in chronic pulmonary inflammation. *J. Exp. Med.* 170:727–735.

15. Raghow, R., P. Irish, and A. H. Kang. 1989. Coordinate regulation of transforming growth factor β gene expression and cell proliferation in hamster lungs undergoing bleomycin-induced pulmonary fibrosis. *J. Clin. Invest.* 84:1836–1842.

16. Czaja, M. J., F. R. Weiner, K. C. Flanders, M. A. Giambrone, R. Wind, L. Biempica, and M. A. Zern. 1989. In vitro and in vivo association of transforming growth factor-β_1 with hepatic fibrosis. *J. Cell Biol.* 108:2477–2482.

17. Perkett, E. A., R. M. Lyons, H. L. Moses, K. L. Brigham, and B. Meyrick. 1990. Transforming growth factor-β activity in sheep lung lymph during the development of pulmonary hypertension. *J. Clin. Invest.* 86:1459–1464.

18. Majesky, M. W., V. Lindner, D. R. Twardzik, S. M. Schwartz, and M. A. Reidy. 1991. Production of transforming growth factor β_1 during repair of arterial injury. *J. Clin. Invest.* 88:904–910.

19. Sarzani, R., P. Brecher, and A. V. Chobanian. 1989. Growth factor expression in aorta of normotensive and hypertensive rats. *J. Clin. Invest.* 83:1404–1408.

20. Stenmark, K. R., J. Fasules, D. M. Hyde, N. F. Voelkel, J. Henson, A. Tucker, H. Wilson, and J. T. Reeves. 1987. Severe pulmonary hypertension and arterial adventitial changes in newborn calves at 4,300 m. *Am. J. Physiol.* 62:821–830.

21. Parks, W. C., H. Secrist, L. C. Wu, and R. P. Mecham. 1988. Developmental regulation of tropoelastin isoforms. *J. Biol. Chem.* 263:4416–4423.

22. Prosser, I. W., K. R. Stenmark, M. Suthar, E. C. Crouch, R. P. Mecham, and W. C. Parks. 1989. Regional heterogeneity of elastin and collagen gene expression in intralobar arteries in response to hypoxic pulmonary hypertension as demonstrated by in situ hybridization. *Am. J. Pathol.* 135:1073–1087.

23. Flanders, K. C., N. L. Thompson, D. S. Cissel, E. Van Obberghen-Schilling, C. C. Baker, M. E. Kass, L. R. Ellingsworth, A. B. Roberts, and M. B. Sporn. 1989. Transforming growth factor-beta 1: histochemical localization with antibodies to different epitopes. *J. Cell Biol.* 108:653–660.

24. Derynck, R., J. A. Jarrett, E. Y. Chen, D. H. Eaton, J. R. Bell, R. K. Assoian, A. B. Roberts, M. B. Sporn, and D. V. Goeddel. 1985. Human transforming growth factor-β complementary DNA sequence and expression in normal and transformed cells. *Nature (Lond.).* 316:701–705.

25. Wrenn, D. S., W. C. Parks, L. A. Whitehouse, E. C. Crouch, U. Kucich, J. Rosenbloom, and R. P. Mecham. 1987. Identification of multiple tropoelastins secreted by bovine cells. *J. Biol. Chem.* 262:2244–2249.

26. Madisen, L., N. R. Webb, T. M. Rose, H. Marquardt, T. Ikeda, D. Twardzik, S. Seyedin, and A. F. Purchio. 1988. Transforming growth factor-beta-2: cDNA cloning and sequence analysis. *DNA (NY).* 7:1–8.

27. ten Dijke, P., P. Hansen, K. Iwata, C. Pieler, and J. G. Foulkes. 1988. Identification of another member of the transforming growth factor type beta family. *Proc. Natl. Acad. Sci. USA.* 85:4715–4719.

28. Jakowlew, S. B., P. J. Dillard, M. B. Sporn, and A. B. Roberts. 1988. Complementary deoxyribonucleic acid cloning of a messenger ribonucleic acid encoding transforming growth factor beta 4 from chicken embryo chondrocytes. *Mol. Endocrinol.* 2:1186–1195.

29. Kondaiah, P., M. J. Sands, J. M. Smith, A. Fields, A. B. Roberts, M. B. Sporn, and D. A. Melton. 1990. Identification of a novel transforming growth factor-beta (TGF-beta 5) mRNA in Xenopus laevis. *J. Biol. Chem.* 265:1089–1093.

30. Sabath, D. E., H. E. Broome, and M. B. Prystowsky. 1990. Glyceraldehyde-3-phosphate dehydrogenase mRNA is a major interleukin 2-induced transcript in a cloned T-helper lymphocyte. *Gene (Amst.).* 91:185–191.

31. Arcari, P., R. Martinelli, and F. Salvatore. 1990. The complete sequence of a full length cDNA for human liver glyceraldehyde-3-phosphate dehydrogenase: Evidence for multiple mRNA species. *Nucleic Acids Res.* 12:9179–9189.

32. Larzul, D., F. Guigue, J. J. Sninsky, D. H. Mack, C. Brechot, and J. L. Guesdon. 1988. Detection of hepatitis B virus sequences in serum by using in vitro enzymatic amplification. *J. Virol. Methods.* 20:227–237.

33. Innis, M. A., and D. H. Gelfand. 1990. Optimization of PCRs. *In* PCR Protocols: A Guide to Methods and Applications. M. A. Innis, D. H. Gelfand, J. J. Sninsky, and T. J. White, editors. Academic Press, Inc., New York. 3–12.

34. McGowan, S. E., and R. McNamer. 1990. Transforming growth factor-β increases elastin production by neonatal rat lung fibroblasts. *Am. J. Respir. Cell Mol. Biol.* 3:369–376.

35. Liau, G., and L. M. Chan. 1989. Regulation of extracellular matrix RNA levels in cultured smooth muscle cells. *J. Biol. Chem.* 264:10315–10320.

36. Roberts, A. B., M. A. Anzano, L. M. Wakefield, N. S. Roche, D. F. Stern, and M. B. Sporn. 1985. Type β transforming growth factor: a bifunctional regulator of cellular growth. *Proc. Natl. Acad. Sci. USA.* 82:119–123.

37. Fine, A., C. F. Poliks, L. P. Donahue, B. D. Smith, and R. H. Goldstein. 1989. The differential effect of prostaglandin E_2 on transforming growth factor-β and insulin-induced collagen formation in lung fibroblasts. *J. Biol. Chem.* 264:16988–16991.

38. Peltonen, J., L. Kahari, S. Jaakkola, V.-M. Kahari, J. Varga, J. Uitto, and S. A. Jimenez. 1990. Evaluation of transforming growth factor β and type I procollagen gene expression in fibrotic skin diseases by in situ hybridization. *J. Invest. Dermatol.* 94:365–371.

39. Majesky, M. W., S. M. Schwartz, M. M. Clowes, and A. W. Clowes. 1987. Heparin regulates smooth muscle S phase entry in the injured rat carotid artery. *Circ. Res.* 61:296–300.

40. Kourembanas, S., R. L. Hannan, and D. V. Faller. 1990. Oxygen tension regulates the expression of the platelet-derived growth factor-B chain gene in human endothelial cells. *J. Clin. Invest.* 86:670–674.

41. Allen, K., and S. G. Haworth. 1988. Human postnatal pulmonary arterial remodeling. *Lab. Invest.* 59:702–709.

42. Hall, S., and S. G. Haworth. 1986. Conducting pulmonary arteries: structural adaption to extra-uterine life. *Cardiovasc. Res.* 21:208–216.